Journal of Molecular Graphics and Modelling 72 (2017) 148–155

Contents lists available at ScienceDirect

Journal of Molecular Graphics and Modelling

journal homepage: www.elsevier.com/locate/JMGM

Study of molecular interactions between Chitosan and Vi Antigen

Natália de Farias Silva[a,b], Raimundo Lopes da Silva[b], Kalene de Oliveira Almeida[b], Antônio Edilson Sousa do Nascimento-Júnior[c], Davi do Socorro Barros Brasil[c], José Otávio Carréra Silva-Júnior[a], Francisco Martins Teixeira[d], Roseane Maria Ribeiro-Costa[b,*]

[a] Laboratory R & D Pharmaceutical and Cosmetic, College of Pharmacy, Federal University of Pará, Belém, Pará, Brazil
[b] Laboratory Quality Control, College of Pharmacy, Federal University of Pará, Brazil
[c] Institute of Technology, Federal University of Pará, Belém, Pará, Brazil
[d] College of Pharmacy, Federal University of Rio of Janeiro, Macaé, Rio de Janeiro, Brazil

ARTICLE INFO

Article history:
Received 13 June 2016
Received in revised form 25 August 2016
Accepted 29 December 2016
Available online 31 December 2016

Keywords:
Vi Antigen
Chitosan
Molecular docking
Adsorption system
Nanoparticles Chitosan-Vi Antigen

ABSTRACT

Chitosan has attracted much interest due to its special physical and chemical properties related to drug administration. Nanoparticles delivery systems from Vi Antigen are a promising approach in the struggle against typhoid fever. In this paper, we reported the obtainment and the characterization of Vi Antigen by Infrared spectroscopy as well as Molecular Modeling and Computational Chemistry studies of the Chitosan-Vi Antigen interaction through theoretical models. The results of the theoretical and experimental Infrared spectroscopy showed important bands related to *N*-Acetyl and *O*-Acetyl groups present in Vi Antigen. Important interactions related to its adsorption were observed through three-dimensional optimized structures. Two models were proposed for the Chitosan-Vi Antigen in adsorption system, one as a monomer and another as an optimized tetrasaccharide antigen. The Molecular Modeling studies presented the best conformation and binding site on the nanoparticle Chitosan-Vi Antigen in models proposed. Interactions were observed between *O*-Acetyl and *N*-Acetyl groups the Vi Antigen and hydroxy, amino and methyl groups the Chitosan.

1. Introduction

In developing regions (Asia, Africa, Central America and South America) typhoid fever is still a serious public health problem, because it leads to death more than 222 000 people every year [1,2]. According to the World Health Organization [3], it is estimated that typhoid fever affects about 21 million people annually, of which around 4% end in death [3,4]. Studies show that the incidence is higher in children aged below two years of age [3,5,6].

The agent responsible for the occurrence of typhoid fever is *Salmonella enterica* serovar Typhi, a gram negative bacillus belonging to the Enterobacteriaceae family, glucose fermenter and which has three antigens: O or somatic antigen, H or flagellar antigen and Vi or capsular antigen, which in turn are of great importance for the diagnosis of typhoid fever. These bacteria are uniquely adapted to mankind, who are their only natural host. They may be transmitted through raw or undercooked food, or even by drinking contaminated water [7–9].

The typhoid fever is an acute bacterial disease related to the endotoxin of the bacteria, with clinical manifestations such as abdominal pain, diarrhea, high fever, rash, papular erythematous lesions; it may reach more severe manifestations such as hepatosplenomegaly, intestinal bleeding and even more rarely, intestinal perforation and femoral thrombosis. In order to reduce transmission and ensure protection of individuals, the scientific community has been working on the development of vaccines containing Vi capsular antigen [7,8,10].

The Vi capsular antigen is a linear a homopolymer of (1 → 4) 2-deoxy-2-*N*-Acetyl galacturonic acid, where the C_3 group is variably *O*-Acetylated [11]. It is able to stimulate the production of antibodies, but the development of vaccines containing this antigen has complications because it is effective only during a short period of immunization, and is unprovided with immunological memory.

Thus, new strategies have been sought as the use of controlled release systems, exemplified by the conjugation of a carrier polysaccharide to a protein or other non-protein antigens. As

* Corresponding author at: Laboratory Quality Control, College of Pharmacy, Federal University of Pará Rua Augusto Corrêa, 01, Guamá, Belém, Pará 66075-170, Brazil.
E-mail address: rmrc@ufpa.br (R.M. Ribeiro-Costa).

http://dx.doi.org/10.1016/j.jmgm.2016.12.015
1093-3263/

an example of a controlled release system we can mention the nanocarriers, such as Chitosan nanoparticles which are able to encapsulate drugs, proteins or antigens, allowing this active agent to be gradually and slowly released [12]. Production of nanoparticles containing the antigen enables the stimulation of the immune system thereby generating a more durable immune response, and aiding in the protection against the bacteria [6,9,10,13,14]. The nanoparticles can be made from synthetic and/or natural polymers; in the latter kind Chitosan is an outstanding amino polysaccharide derived from the deacetylation process of the chitin considered a copolymer with 2-amino-2-deoxy-D-glucose and 2-acetamide-2-deoxy-D-glucose units, which are joined by glycosidic linkages of the type $\beta(1 \rightarrow 4)$ with its structure C_6 being composed of a primary amino group and two free hydroxyl groups [15,16].

Interest in controlled release systems has increased in recent years, and consequently, the search to improve this system. Computational Chemistry is emerging as an alternative for understanding the nanocapsules or nanospheres encapsulation, as well as their adsorption and release system [17]. The use of focused computer programs to study the chemical and networked databases are currently important tools for drug discovery and design [18]. These theoretical methods help in the identification and preparation of biologically active compounds through studies related to their structure, activity, metabolism, as well as their mechanism of action [19]. In Computational Chemistry, Molecular Modeling consists in creating theoretical models, in atomistic scale, which describe or interpret macroscopic properties that lead to improved absorption kinetics of a drug or the mechanism of action of a substrate [18,19]. Molecular Modeling through computer softwares makes it possible to study the physicochemical properties and the three-dimensional visualization of the molecular steroelectronic properties, as well as the elucidation of the interaction between drug and target macromolecules [19].

In this work, the Vi Antigen of *Salmonella* Typhi was extracted, purified and identified by Infrared Spectroscopy. The theoretical infrared spectra of the Vi Antigen was calculated and compared to the experimental. Additionally, the theoretical study was proposed to assess the intramolecular interactions between Chitosan and the Vi Antigen. The results of this study can be used as support for future development of vaccines against typhoid fever.

2. Experimental section

2.1. Materials and reagents

A strain of *Salmonella enterica* serotype Typhi was kindly provided by the Instituto Nacional de Controle de Qualidade em Saúde (INCQS) from the Oswaldo Cruz Foundation (FIOCRUZ). Sodium azide, hexadecyltrimethylammonium bromide, deoxyribonuclease and ribonuclease were supplied by Sigma Aldrich® (Germany). Tris (hydroxymethyl) aminomethane was acquired from Cientifica® Passos (São Paulo).

2.2. Obtaining strains

Lyophilized strains of *Salmonella* Typhi were resuspended in 1 mL of nutrient broth and streaked in *Salmonella-Shigella* Agar to its best growth. Grown bacteria were subjected to biochemical and serological tests to confirm the presence of Vi Antigen and then stored in Agar nutrient in the refrigerator for later use.

2.3. Vi capsular antigen extraction from Salmonella Typhi

Wong and Feeley technique [20] was adapted to perform the extraction using multiple reagents and multiple centrifugations. For a considerable bacterial mass, an isolated colony of the stored strains of *Salmonella* Typhi, was streaked in TSB broth, for an exponential growth and then transferred to Agar nutrient in a glass bottle, and left for 24 h. After that time the mass of bacteria was extracted from the flask and stored in 50 mL Falcon tubes. The bacterial cells were killed before the antigen isolation; the same technique employed by Wong et al. [21]. The antigen isolation began with the addition of 0.1% sodium azide solution in the killed cells, and stirred in water bath for 30 min and then centrifuged at 11,000 rpm for 30 min. Centrifugation finished, the supernatant was isolated and transferred to another Falcon tube.

To the supernatant, 1 mL of Tris-HCl buffer and 500 μL of ribonuclease and deoxyribonuclease enzymes were added and placed under stirring for 6 h at 37 °C. After this time 500 μL of pronase was added and stirred for 12 h. Subsequently, NaCl 5% (w/v) was added and the mixture was stowed in the freezer until freezing. Then 6 mL of pre-cooled ethanol was added and kept in the refrigerator overnight.

This mixture was centrifuged for 30 min at 11,000 rpm and then the pellet was isolated, and 5 mL of 60% ethanol in saline solution was added and stirred for 24 h. After this period, the supernatant was centrifuged and extracted. This process was performed twice more to yield a supernatant pool.

The supernatant was frozen at 2 °C and then an equal volume of pre-chilled ethanol was added and the mixture was kept in the refrigerator for 15 min. Subsequently, it was subjected to centrifugation of 11000 rpm at 2 °C for 30 min. The pellet was isolated and 10 mL of sterile 0.85% saline solution and 0.01 g of hexadecyltrimethylammonium bromide (w/v) were added and centrifuged at 8000 rpm for 15 min; 4 mL of 1 M KCl solution was added to the isolated sediment and then this mixture was filtered through 30.000 KDa ultra thin millipore filter. The tube containing the mixture was submitted to centrifugation of 7000 rpm for 15 min for an efficient filtration.

The recovery of the antigen retained on the filter was performed by the dropwise addition of 2 mL of ethanol PA and centrifuged at 8000 rpm for 20 min. The sediment which contained the antigen was removed and 5 mL of saline solution and 2 mL of ethanol PA were added, obtaining a suspension of the antigen. The suspension was lyophilized and stored for use in later techniques.

2.4. Infrared technique in Vi Antigen identification

Infrared spectroscopy in antigen identification is one of the most important and well applied analytical techniques. In this study, we used this technique of Fourier transforms to identify the characteristic functional groups of the Vi Antigen. The lyophilized sample obtained from the isolation and purification method, was sprayed with 99 mg of potassium bromide (KBr) and subjected to a high pressure to form the tablet. The spectra were obtained on a Shimadzu IRPrestige-21® spectrophotometer, in the wavelength range from 4000 to 400 cm^{-1} during 32 scans with a resolution of 4 cm^{-1}.

2.5. Computational session

In order to have a better understanding of the interaction between Chitosan and the Vi capsular antigen, a Molecular Modeling study of these structures was performed to comprehend the possible interactions between Chitosan and Vi Antigen during adsorption process and thus its stability. The structures were initially treated separately. The three-dimensional (3D) structure of the Chitosan was obtained from the NCBI (National Center for Biotechnology Information), which had the monomer and its molecular structure. As for the Vi Antigen we used the postulated model from the study by Yang et al. [22] using the monomer and tetrassacharide derived from the antigen, where the structure was generated using the ChemDraw Ultra 12 software (CambridgeSoft

Corporation, Cambridge, MA) and subsequently the 3D structure was obtained (CambridgeSoft Corporation, Cambridge, MA). Then the Chem3D 12 program was used to perform a conformational search in order to convert it into a three-dimensional (3D) structure, plus the addition of hydrogens. The same procedure was performed both for Chitosan and Vi Antigen structures. To solve the problem of conflicting charges the structures were subjected to DFT calculations using the B3PLYP hybrid functional [23,24] and the 6-31G(d,p) basis set in the Gaussian 03 program [25]. In order to compare experimental data obtained by extraction and purification of the Vi Antigen, infrared theoretical calculations using B3PLYP together with 6-31G(d,p) basis set and semi-empirical with methods AM1 and PM3 were carried out in the Gaussian 03 program [25]. Energy values as well as infrared theoretical calculations were obtained using the Gaussian 03 program package [25]. The frequencies calculations were also calculated using B3LYP/6-31G(d,p), and observed that there were no negative frequencies, thereby ensuring that local minimum energy structures.

The Molecular Electrostatic Potential (MEP) has been applied in the study of biological interactions and the definition of molecular reactivity patterns [26,27]. This is a highly informative tool for the distribution of electronic and nuclear charges of a given molecule. Herein, the surfaces of MEP were derived from the B3LYP/6-31G(d,p) method calculated on Gaussian 03 program [25] and visualized in Molekel Molecular Visualization [28]. These surfaces correspond to an isodensity value of 0.05 a.u. The MEP was carried out to study the important regions of the Vi Antigen and to try to correlate them with their biological activity.

The Molecular Docking studies were performed with the AutoDock 4.2 software [29] for the two proposed models using regular precision with a maximum of 100 conformations per candidate. Kollman charges and hydrogens necessary for the calculation were added in the Chitosan molecule. The rotational links of binders were automatically set and their non-polar hydrogens removed. Conformations were classified using the Scoring function and Genetic Lamarckian Algorithm. After the location of potential binding sites, the Chitosan-antigen complex conformations were optimized using the steepest decent algorithm to convergence with a maximum of 10 iterations.

3. Results and discussion

3.1. Infra-Red spectroscopy to Vi Antigen

In this work the analysis of the extracted and purified Vi Antigen and commercial Vi Antigen were performed. The FTIR spectra of the extracted and commercial Vi Antigen can be viewed in Fig. 1. The commercially pure antigen spectrum showed a peak at 617 cm^{-1} due to vibrations of the piranosidic ring, common in polysaccharides, a shifting between 1200 and 950 cm^{-1}, corresponding to the C—O—C stretching; and a peak at 1734 cm^{-1}, related to *O*-Acetyl group [11] (Fig. 1). Still for the commercial antigen spectrum, an adsorption band between 1650 and 1540 cm^{-1} was observed, which corresponds to the *N*-acetamide group; and between 1604 and 1417 cm^{-1} related to the presence of carboxylate anion (Fig. 1). The presence of *O*-Acetyl and *N*-Acetyl groups in the Vi Antigen structure is important, since studies relate these groups with immunochemical properties of the antigen in *Salmonella enterica* serotype Typhi Ty2 [30]. In the extracted and purified antigen, there was a similar peak at 617 cm^{-1}, corresponding to the vibrations of the piranosidic ring, as well as the band at 1101 cm^{-1} due to the C—O—C stretching, and between 1650 and 1540 cm^{-1}, due to the *N*-Acetyl group (Fig. 1). The range between 1604- 1417 cm^{-1} corresponded to the carboxylate anion. Yet the presence of the band at 1734 cm^{-1} was detected, related to *O*-Acetyl group (Fig. 1). It is also

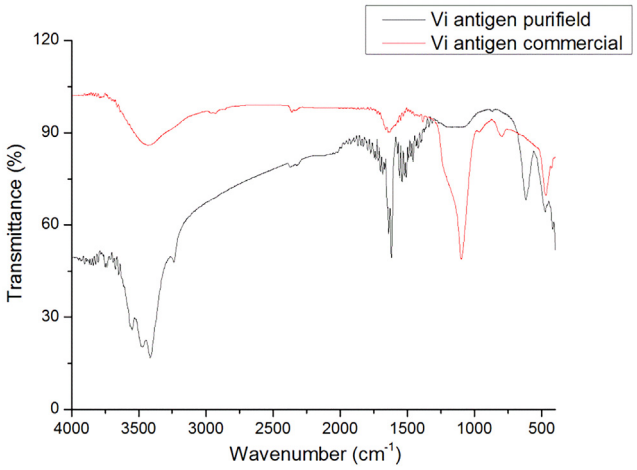

Fig. 1. FTIR spectrum for Purified and Commercialized Vi Antigen.

important to note the presence of an intense and rather sharp band attributed to the carboxylic group, which is part of the polysaccharide structure, which may be important in a possible connection of this group to antibodies. Soares observed regions corresponding to the carboxylic acid between 1650 and 1630 cm^{-1} for polysaccharides fractions extracted from seaweed [31]. However, Santos et al. [32] noticed the presence of carboxylic acid between 1629 and 1618 cm^{-1} in *Campomanesia xanthocarpa* Berg polysaccharide fractions. Other studies have reported values close to those found in this work for the piranosidic ring. Moura found the corresponding peak at 620 cm^{-1} for the piranosidic ring of Chitosan, in nanoparticles production [33]. Mallmann showed the presence of a band with a result from 1200 to 800 cm^{-1} in studies of the same substance for obtaining biological compounds with magnetic properties [34]. The spectrum behavior for the extracted antigen was similar to the commercial antigen, both showed the same typical groups, which demonstrates that during the extraction process there was no loss of groups that will create the immunity of the antigen. The values of the bands to extracted and purified and commercial Vi Antigen are shown in Table 1.

The IR spectroscopy technique was crucial to prove that the antigen was extracted correctly and for comparison with the IR theoretical validating Molecular Modeling study. From the optimized structures of Vi Antigen, the IR theoretical calculations were performed using three types of methods: B3LYP, AM1 and PM3. These spectra can be seen in Fig. 2. According to these results, it can be observed that the theoretical methodology can satisfactorily describe the experimental one. Analysis of Fig. 2 shows that stretches from the groups *O*-Acetyl and *N*-Acetyl which are characteristic of the Vi Antigen, are well noted by all theoretical methods applied here. Another stretch quite observed was the C—O—C stretch and those belonging to the carboxylic acid. We noted that for the results with the B3LYP method (Fig. 2a), the presence of bands at 1518 cm^{-1} related to the *N*-Acetyl group and at 1808 cm^{-1} to the *O*-Acetyl group were detected. It was also observed a band at 973 cm^{-1} which corresponds to the C—O—C stretching. A peak of 659 cm^{-1} was attributed to the vibrations of the piranosidic ring. In the results with the AM1 method (Fig. 2b) the bands related to *N*-Acetyl and *O*-Acetyl groups were noted again at 1654 cm^{-1} and 1517 cm^{-1}, respectively. The C—O—C stretch was observed at 927 cm^{-1}. A peak at 659 cm^{-1} was attributed to the vibrations of the piranosidic ring. As for the PM3 method (Fig. 2c), the presence of the band at 1575 cm^{-1} was attributed to the *N*-Acetyl group. The presence of a peak at 855 cm^{-1} was related to the C—O—C stretching. The results obtained by theoretical methods to the optimized structures of Vi Antigen are shown in Table 1. The

Table 1
Theoretical and experimental assignments of infrared absorption bands (cm^{-1}).

Vibrational modes	Commercial Vi Antigen	Purified Vi Antigen	B3LYP/6-31G (d,p)	AM1	PM3
Piranosidic ring	617	617	659	659	682
O-Acetyl group	1734	1734	1808	1517	
N-Acetyl group	1650–1540	1650–1540	1518	1654	1575
C—O—C	1200–950	1101	973	927	855
Carbolylate anion	1604–1417	1604–1417			

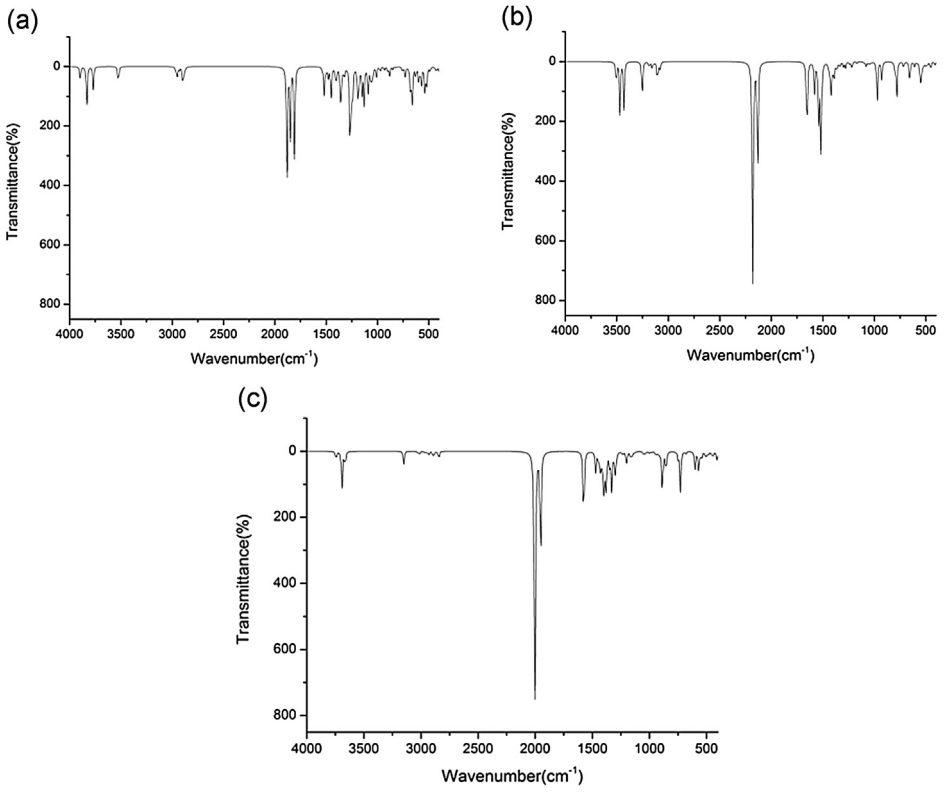

Fig. 2. Theoretical spectrum of Vi Antigen at (a) B3LYP/6-31G(d,p), (b) AM1 and (c) PM3 levels.

analysis in Fig. 2 shows that when comparing the three methods, the B3LYP was the one that best described the Vi Antigen structure, which is consistent with the experimental results presented in Fig. 1.

3.2. Vi Antigen model

The Vi Antigen stability study (a homopolymer with α (1 → 4) linked) started from its previous structure defined in the literature, where the arrangements of the *N*-Acetyl, *O*-Acetyl, hydroxyl groups, and the carboxylic group are already shown for the theoretical study. The study of the monomer involved conformational analysis evaluating the angles and atoms and groups bonds. All calculations used the DFT methodology with B3LYP functional and 6-31G(d,p) basis set. As noted, the bonds between the carbon, nitrogen, oxygen and hydrogen atoms are within the expected values for polymers. The optimized resulting structure can be seen in Fig. 3a. The bonds observed in the piranosidic ring between C—C groups had a value of 1.52 Å, whereas the bond C—O presented a value of 1.41 Å. In the *N*-Acetyl group, the bond C—N had a value of 1.47 Å, while the bond C—O in the group O—N exhibited a value of 1.40 Å. For the remaining bonds C—H, C=O and O—H values of 1.11 Å, 1.21 Å and 0.97 Å were observed, respectively. Other important points analyzed in Vi Antigen-monomer were bond angles and the dihedral angle formed in the piranosidic ring and in the groups

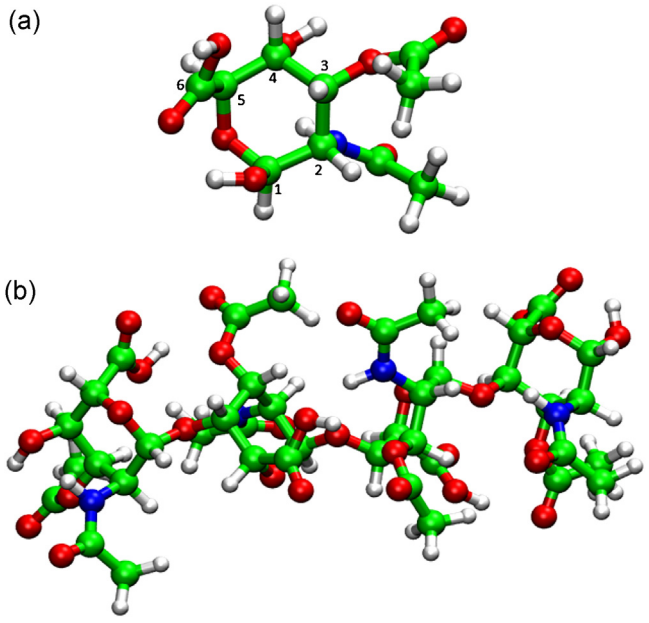

Fig. 3. Snapshot representative for (a) monomer and (b) tetrasaccharide Vi Antigen obtained after optimization.

Table 2
Theoretical structural parameters for Vi Antigen.

Structural Parameter	B3LYP/6-31G(d,p)
Distance bonds (Å)	
C—C (ring)	1.52
C—O (ring)	1.41
C—N (*N*-Acetyl group)	1.47
C—O (*O*-Acetyl group)	1.40
C=O	1.21
C—H	1.11
C=O	0.97
Bond angles (°)	
C—N—C (*N*-Acetyl group)	126.50
C—O—C (*O*-Acetyl group)	13.92
O—C_5—C_4	113.10
C_1—O—C_5	109.88
Dihedral angles (°)	
C_2—N—O_3—C_7 (*N*-Acetyl group)	5.71
C_3—O_4—O_5—C_8 (*O*-Acetyl group)	2.18
O—C_1—C_2—C_3	−52.58

N-Acetyl and *O*-Acetyl, since the presence and correct description of this group is directly linked to the Antigen immunity. The dihedral angle formed in the group *N*-Acetyl (C_2—N—O_3—C_7) showed a value of 2.18°, while for *O*-Acetyl group the angle observed was of 5,71° formed by C_3—O_4—O_5—C_8. In the piranosidic ring, the dihedral angle formed between O—C_1—C_2—C_3 was of −52.58°. The bond angles for *N*-Acetyl and *O*-Acetyl groups showed values of 126.50° and 13.92° respectively. Bond angles of 113.10° were observed for the piranosidic ring between O—C_4—C_5 and between C_1—O—C_5 with value of 109.88°. These and other results are shown in Table 2.

Regarding the most stable conformation of the monomer, optimization studies of minimization started, as to create the adsorption models of Chitosan. According to Yang et al., structures containing derivatives of Vi Antigen with tri and tetrasaccharide showed better inhibition results in ELISA test [22]. Thus, the structure was designed, optimized and minimized by DFT method with B3LYP functional and 6-31G(d,p) basis set. The resulting structure of this optimization can be seen in Fig. 3b. According to the results, some changes were found in the monomer, since it has a greater number of atoms around, a new rearrangement is required so that the final system is stable. The bonds between the carbon, nitrogen, oxygen and hydrogen atoms showed values found in the monomer. An important fact to be noted is that the model consists of four monomer units, therefore, the groups *N*-Acetyl and *O*-Acetyl together with the carboxylic group had some changes in the bond and dihedral angles to obtain the most stable conformation. Other interactions were observed for this model. Intramolecular interactions among groups stabilized the model and can be viewed in Fig. 3c. A strong hydrogen bond of 2.10 Å is formed between the hydrogen of the carboxylic acid and the oxygen of the carboline from the *O*-Acetyl group in the first monomer of this model. As for the second and third monomer, hydrogen bonds are observed between the hydrogen of the *N*-Acetyl group and the oxygen of the piranosidic ring. The observed values were 2.08 Å and 2.15 Å, respectively. Finally, in the last monomer, a hydrogen bonding of 2.17 Å between H of the *N*-Acetyl group and the oxygen of the hydroxyl group from the piranosidic ring was observed.

The MEP surfaces were computed in order to understand important regions of the Vi Antigen and correlate them with their biological activity. Fig. 4 shows the surfaces of the MEPs for Vi Antigen monomer and tetrasaccharide, where the nucleophilic regions (negative electrostatic potential) are shown in red and the electrophilic regions (positive electrostatic potential) are shown in blue. Analysis of the MEP shown in Fig. 4a reveals a region of negative electrostatic potential around the oxygen atoms, especially from the *O*-Acetyl group and the hydroxyl group of the carboxylic acid. It is also observed a negative potential region in the piranosidic ring. These results demonstrate that these regions tend to have stronger interactions. The highlight of these regions in the molecule indicates the region with higher probability of perform nucleophilic attack, in this study, in the amino groups in chitosan nanocapsule during adsorption process. Regions with positive potential for Vi Antigen can be observed around hydrogen atoms of the *N*-Acetyl group. The evidence of these regions characterizes the portion having a higher probability to suffer nucleophilic attack by hydroxy groups presents in Chitosan nanocapsule. Others interactions can be observed for tetrasaccharide (Fig. 4b), region of negative electrostatic potential around the oxygen atoms of the *O*-Acetyl and *N*-Acetyl group results in regions with stronger interactions, which demonstrates that these regions in the tetrasaccharide with higher probability of perform nucleophilic attack, in the amino groups in Chitosan nanocapsule. Larger positive electrostatic potentials can be found around the hydrogen atom of the *N*-Acetyl groups, which also showing higher probability to suffer nucleophilic attack by hydroxy groups presents in Chitosan nanocapsule during adsorption process. The presence of the *O*-Acetyl and *N*-Acetyl group are very importance to biological activity of the Vi Antigen and their interactions with groups, as in the study, amino and hydroxy groups presents in the Chitosan are closely related to the development of this activity. The analysis of MEPS demonstrates the great importance of detailing the interactions of these groups in the Chitosan nanocapsule during adsorption process.

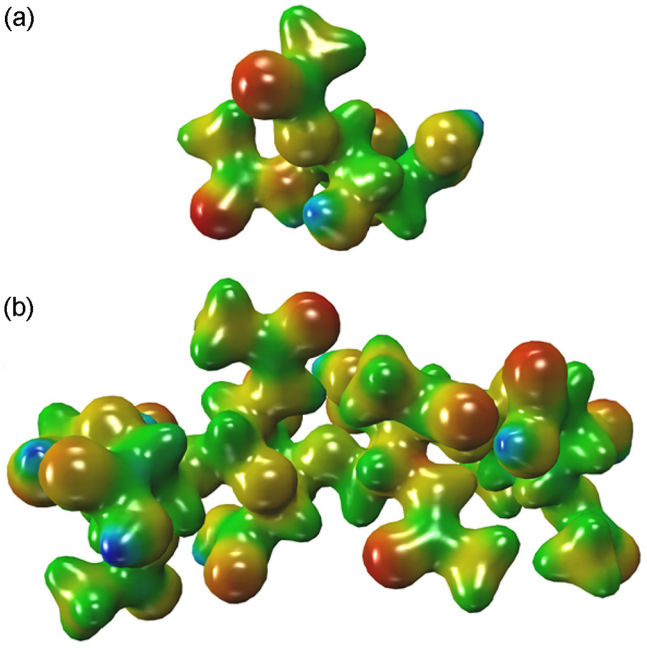

Fig. 4. Map electrostatic potential (MEP) surfaces derived from B3LYP/6-31G(d,p) calculations for (a) monomer and (b) tetrasaccharide Vi Antigen. The increase of negative charges goes from the blue (positive) to red (negative).

3.3. Chitosan-Vi Antigen Models

The activities of *N*-Acetyl and *O*-Acetyl groups on the tetrasaccharide model was significant by Elisa test, since these groups have played a dominant role in the determination of antigenic activity when compared to that previously reported in the literature [35]. These proposed theoretical models containing the monomer and the tetrasaccharide show contrary behavior pattern of these structures to other biomacromolecules, such as Chitosan nanoparticles in an adsorption system. Because of this fact, the study of interactions in Chitosan nanoparticles is an important key to under-

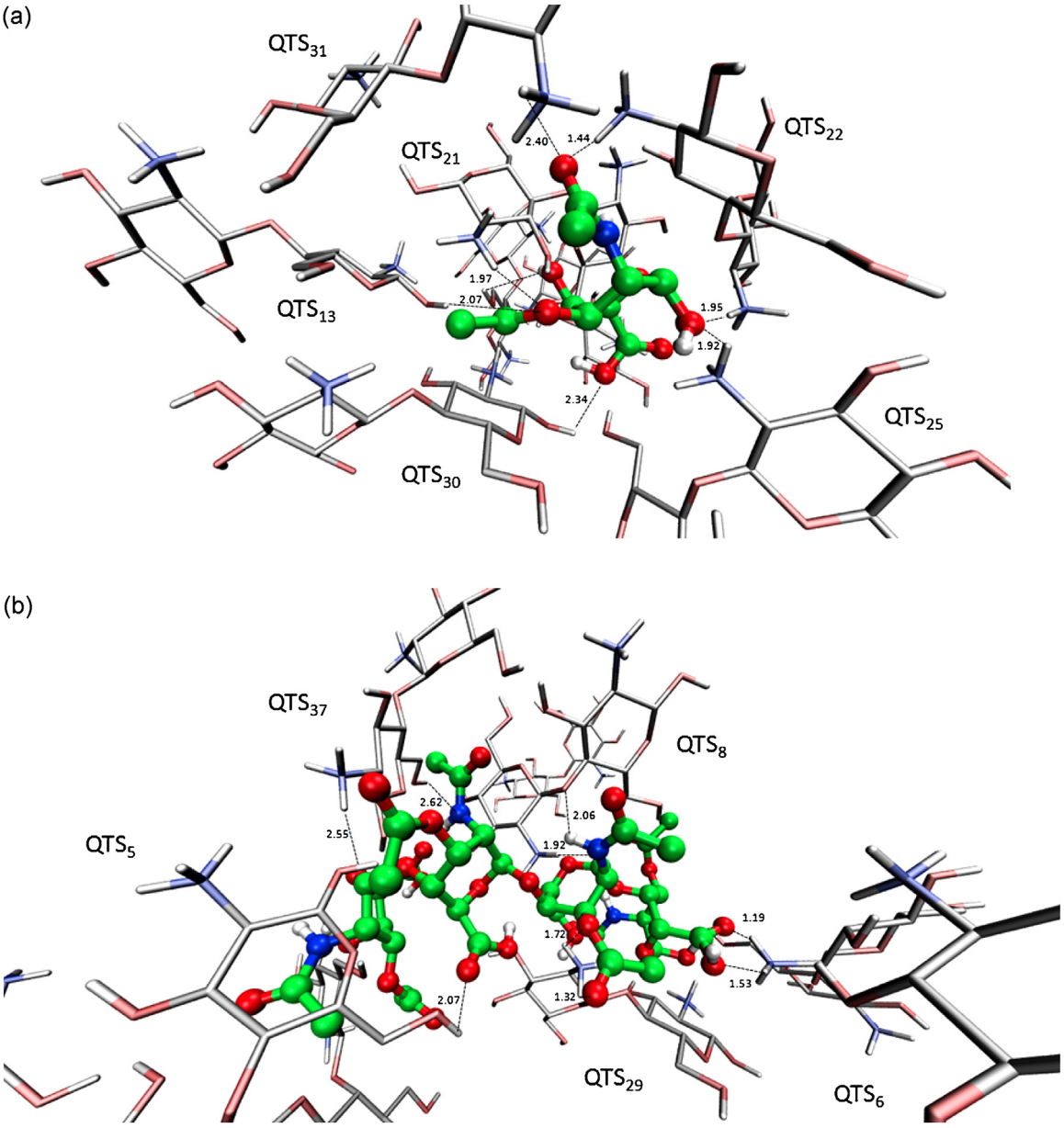

Fig. 5. The result of docking conformation obtained for (a) model 1 and (b) model 2 in Chitosan nanoparticles with Vi Antigen.

standing its biological activity. In order to study the interactions established between Vi Antigen and Chitosan we suggest the construction of theoretical models by Computational Chemistry and Molecular Modeling, to have a better comprehension and representation of a Chitosan nanocapsule. These models start from already optimized structures and therefore require low computational cost. The models were created with the aid of Packmol software [36], with the advantage of being free and fast for the creation of thousands of atoms models. For this initial analysis, the interface system was chosen to describe the Chitosan-antigen interaction. Two models were analyzed; the first with a Chitosan interface containing an amount of 40 monomers and 1 Vi Antigen monomer interleaved, in a total amount of 80 Chitosan structures. The second model contained the same amount of Chitosan, 80 structures and 4 monomers of the Vi Antigen interleaved. The model haying the monomer structure (Model 1) was initially proposed to understand the interactions of *N*-Acetyl and *O*-Acetyl groups on the Chitosan nanoparticles and the model cotaning the tetrasaccharide proposed by Yang et al. [22] (Model 2) showed an improved antigenic activity in ELISA test associated with increased *O*-Acetyl and *N*-Acetyl groups. To verify this information, these two theoretical models of nanoparticles containing the monomer and the tetrasaccharide Vi Antigen have been proposed with the use of the Molecular Modeling to associate and explain the interactions that occur between these structures. The proposed models can be viewed in Supplementary Information. The results show that the creation of the interface both for Model 1 and Model 2 was quite satisfactory; there was no clash between the antigen and Chitosan atoms.

The results obtained by Packmol software were used to predict the form of docking between the structure of the monomer and Vi Antigen tetrasaccharide with Chitosan molecules that form the nanoparticle to determine the best conformation and binding site on the nanoparticle. Sanyakamdhorn et al. reported docking studies for to determine the preferred biding site on the chitosan to Dox and FDox molecules [17]. The results show that the docking for both proposed models showed Vi Antigen surrounded by the Chitosan molecules stabilizing the complex. For Model 1 an energy value of 39.2 kcal mol^{-1} was observed, while for Model 2 the value

was 166 kcal mol^{-1}. This energy difference is attributed to a larger amount of atoms in the structure of the antigen in Model 2, as it presents four monomers which provide an increase of energy and thus making it less stable when compared to Model 1. The models obtained by Molecular Docking for the studied models are shown in Fig. 5. Looking at Fig. 5a a formation of hydrogen bonds between the Vi Antigen and Chitosan molecules that are closer can be seen. Interactions are established between oxygen atoms from *O*-Acetyl group of the Vi Antigen with amino group and one hydroxy group of Chitosan in values of 2.63 Å and 2.34 Å, respectively. The *N*-Acetyl group of the Vi Antigen also presented a hydrogen bond with two amino groups of Chitosan in values of 2.40 Å and 1.44 Å, respectively. Another hydrogen bond was formed between the hydroxyl oxygen and the amino group of the two Chitosan in values of 1.95 Å and 1.92 Å, respectively. The Oxygen atoms O_3 and O_4 of the Vi Antigen also established hydrogen bonding with the hydroxyl and amino groups of Chitosan molecules in values of 2.07 Å, 1.49 Å and 1.97 Å, respectively. The hydroxyl group of Chitosan also formed a hydrogen bond with the hydrogen atom of the monomer of the Vi Antigen in the value of 2.64 Å. As for Fig. 5b, it is possible to observe that most of the bonds formed in Model 1 are repeated in Model 2; since the monomeric units of the Vi Antigen increase, some of them were expected to repeat. It is important to outstand that the interactions observed in *O*-Acetyl and *N*-Acetyl groups remained in Model 2; values from 1.32–172 Å were observed in the hydrogen bonds established between the groups *O*-Acetyl and amino of Chitosan. As for the *N*-Acetyl group values from 1.92 to 2.62 Å in hydrogen bonds with the amino group and hydroxyl were observed. The amino group of Chitosan formed a hydrogen bond with the *O*-Acetyl in the value of 2.04 Å. The hydroxyl group of Chitosan also formed a hydrogen bond with the carboxylic group in the value of 2.07 Å. Another interaction is established between the oxygen atom and the amino group of Chitosan in value of 2.55 Å. The amino group of Chitosan also formed a hydrogen bond with the oxygen atom and hydroxyl group of Chitosan in values of 1.19 Å and 1.53 Å, respectively. Experimental studies conducted by Yang et al. demonstrated that the tetrasaccharide antigen (Model 2) showed a greatly improved antigenic activity when compared to previous data in literature reports [35]. Various interactions between the *N*-Acetyl *O*-Acetyl groups and Chitosan molecules can be seen in Model 1 and 2 from the Molecular Docking results. The interactions formed are hydrogen bonds between *N*-Acetyl and *O*-Acetyl groups with amino hydroxyl groups present in the Chitosan molecules, and they are responsible for the performance of the biological activity during the adsorption process in the Chitosan nanoparticles system.

4. Conclusion

In conclusion, we reported a study of extraction and characterization of Vi Antigen by Infrared spectroscopy technique. Molecular Modeling and Computational Chemistry studies were also carried out for the monomeric structure and the Vi Antigen tetrasaccharide. Important bands characteristics of the antigen were observed. Important nucleophilic and electrophilic regions were evidenced through the MEP. Finally, two models have been proposed for the adsorption between the antigen and Chitosan. The models were satisfactory and may be used in the next stages of computer simulation.

Acknowledgements

We would like to thank the, Pró-Reitoria de Pesquisa de Pós-Graduação of Universidade Federal do Pará (PROPESP-UFPA) for financial support. Silva, N. F. thanks the Coordenação de Aperfeiçoamento de Pessoal de Nível Superior (CAPES) and Programa de Pós-Graduação em Ciências Farmacêuticas for financial support.

Appendix A. Supplementary data

Supplementary data associated with this article can be found, in the online version, at http://dx.doi.org/10.1016/j.jmgm.2016.12.015.

References

[1] J. Wain, R.S. Hendriksen, M.L. Mikoleit, K.H. Keddy, R.L. Ochiai, Typhoid fever, Lancet 385 (2016) 1136–1145, http://dx.doi.org/10.1016/S0140-6736(13)62708-7.
[2] K.A. Date, A. Bentsi-Enchill, F. Marks, K. Fox, Typhoid fever vaccination strategies, Vaccine 33 (Suppl. 3) (2015) C55–C61, http://dx.doi.org/10.1016/j.vaccine.2015.04.028.
[3] World Health Organization (WHO), Typhoid fever, 2014.
[4] V. Mogasale, B. Maskery, R.L. Ochiai, J.S. Lee, V.V. Mogasale, E. Ramani, Y.E. Kim, J.K. Park, T.F. Wierzba, Burden of typhoid fever in low-income and middle-income countries: a systematic, literature-based update with risk-factor adjustment, Lancet Global Health 2 (2016) e570–e580, http://dx.doi.org/10.1016/S2214-109X(14)70301-8.
[5] J.A. Crump, S.P. Luby, E.D. Mintz, The global burden of typhoid fever, Bull. World Health Organ. 82 (2004) 346–353, http://dx.doi.org/10.1590/S0042-96862004000500008.
[6] S.J. An, Y.K. Yoon, S. Kothari, N. Kothari, J.A. Kim, E. Lee, D.R. Kim, T.H. Park, G.W. Smith, R. Carbis, Physico-chemical properties of Salmonella typhi Vi polysaccharide-diphtheria toxoid conjugate vaccines affect immunogenicity, Vaccine 29 (2011) 7618–7623, http://dx.doi.org/10.1016/j.vaccine.2011.08.019.
[7] E.C.B. Loureiro, N.D.B. Marques, F.L. de P. Ramos, E.M.F. dos Reis, D. dos P. Rodrigues, E. Hofer, Sorovares de Salmonella de origem humana identificados no Estado do Pará, Brasil, no período de 1991 a 2008, Revista Pan-Amazônica de Saúde 1 (2010) 93–100, http://dx.doi.org/10.5123/S2176-62232011000010014.
[8] Ministério da Saúde, Manual integrado de vigilância e controle da febre tifoide, 2008.
[9] R.F.O. Azze, J.C.M. Rodriguez, M.G. Iniesta, X.R.F. Marchena, V.M.R. Alfonso, F.T.S. Padron, Immunogenicity of a new Salmonella Typhi Vi polysaccharide vaccine–vax-TyVi–in Cuban school children and teenagers, Vaccine 21 (2003) 2758–2760, http://dx.doi.org/10.1016/s0264-410x(03)00177-4.
[10] F. Micoli, S. Rondini, I. Pisoni, D. Proietti, F. Berti, P. Costantino, R. Rappuoli, S. Szu, A. Saul, L.B. Martin, Vi-CRM 197 as a new conjugate vaccine against Salmonella Typhi, Vaccine 29 (2011) 712–720, http://dx.doi.org/10.1016/j.vaccine.2010.11.022.
[11] A.L. Stone, S.C. Szu, Application of optical properties of the Vi capsular polysaccharide for quantitation of the Vi antigen in vaccines for typhoid fever, J. Clin. Microbiol. 26 (1988) 719–725.
[12] R.L. da Silva, Sistema de Liberação Controlada de Quitosana contendo o Antígeno Capsular Vi de Salmonella Typhi, Universidade Federal do Para, 2012, http://repositorio.ufpa.br/jspui/handle/2011/5625.
[13] L. Hessel, H. Debois, M. Fletcher, R. Dumas, Experience with Salmonella typhi Vi capsular polysaccharide vaccine, Eur. J. Clin. Microbiol. Infect. Dis. 18 (1999) 609–620, http://dx.doi.org/10.1007/s100960050361.
[14] J.B. Robbins, R. Schneerson, S.C. Szu, A. Fattom, Y. Yang, T. Lagergard, C. Chu, U.S. Sorensen, Prevention of invasive bacterial diseases by immunization with polysaccharide-protein conjugates, Curr. Top. Microbiol. Immunol. 146 (1989) 169–180, http://dx.doi.org/10.1007/978-3-642-74529-4_18.
[15] M. George, T.E. Abraham, Polyionic hydrocolloids for the intestinal delivery of protein drugs: alginate and chitosan—a review, J. Control. Release 114 (2006) 1–14, http://dx.doi.org/10.1016/j.jconrel.2006.04.017.
[16] N. Pacheco, M. Garnica-Gonzalez, M. Gimeno, E. Bárzana, S. Trombotto, L. David, K. Shirai, Structural characterization of chitin and chitosan obtained by biological and chemical methods, Biomacromolecules 12 (2011) 3285–3290, http://dx.doi.org/10.1021/bm200750t.
[17] S. Sanyakamdhorn, D. Agudelo, H.-A. Tajmir-Riahi, Encapsulation of antitumor drug doxorubicin and its analogue by chitosan nanoparticles, Biomacromolecules 14 (2013) 557–563, http://dx.doi.org/10.1021/bm3018577.
[18] T. Schlick, Molecular Modeling and Simulation: An Interdiciplinary Guid., 2nd ed., New York, 2012.
[19] N. de, F. Silva, J. Lameira, C.N. Alves, S. Marti, Computational study of the mechanism of half-reactions in class 1A dihydroorotate dehydrogenase from Trypanosoma cruzi, Phys. Chem. Chem. Phys. 15 (2013) 18863–18871, http://dx.doi.org/10.1039/C3CP52692E.
[20] K.H. Wong, J.C. Feeley, Isolation of Vi antigen and a simple method for its measurement, Appl. Microbiol. 24 (1972) 628–633, http://www.ncbi.nlm.nih.gov/pmc/articles/PMC380626/.
[21] K.H. Wong, J.C. Feeley, M. Pittman, Effect of a Vi-degrading enzyme on potency of typhoid vaccines in mice, J. Infect. Dis. 125 (1972) 360–366, http://dx.doi.org/10.1093/infdis/125.4.360.

[22] L. Yang, J. Zhu, X.-J. Zheng, G. Tai, X.-S. Ye, A highly α-stereoselective synthesis of oligosaccharide fragments of the Vi antigen from Salmonella typhi and their antigenic activities, Chem. Eur. J. 17 (2011) 14518–14526, http://dx.doi.org/10.1002/chem.201102615.
[23] A.D. Becke, Density-functional thermochemistry. III. The role of exact exchange, J. Chem. Phys. 98 (1993) 5648–5652, http://dx.doi.org/10.1063/1.464913.
[24] C. Lee, W. Yang, R.G. Parr, Development of the Colle-Salvetti correlation-energy formula into a functional of the electron density, Phys. Rev. B 37 (1988) 785–789, http://dx.doi.org/10.1103/PhysRevB.37.785.
[25] G.E. Frisch, M. J., Trucks, G. W., Schlegel, H. B., Scuseria, J. Robb, M. A., Cheeseman, J. R., Montgomery, J. A., J.M. I. Vreven, T., Kudin, K. N., Burant, J. C., Millam, M. S. S. S., Tomasi, J., Barone, V., Mennucci, B., Cossi, M. G., Rega, N., Petersson, G. A., Nakatsuji, H., Hada, M. Ehara, M., Toyota, K., Fukuda, R., Hasegawa, J., Ishida, M. L. Nakajima, T., Honda, Y., Kitao, O., Nakai, H., Klene, C. X., Knox, J. E., Hratchian, H. P., Cross, J. B., Adamo, O. Jaramillo, J., Gomperts, R., Stratmann, R. E., Yazyev, J.W. A. Austin, A. J., Cammi, R., Pomelli, C., Ochterski, P. D. P. Y., Morokuma, K., Voth, G. A., Salvador, A.D. S. J. J., Zakrzewski, V. G., Dapprich, S., Daniels, A. D. R. M. C., Farkas, O., Malick, D. K., Rabuck, A. G. K., Foresman, J. B., Ortiz, J. V., Cui, Q, Baboul, G. L. Clifford, S, Cioslowski, J., Stefanov, B. B., Liu, D.J. K. A., Piskorz, P., Komaromi, I., Martin, R. L., Fox, A. C. T., Al-Laham, M. A., Peng, C. Y., Nanayakkara, W. W. M., Gill, P. M. W., Johnson, B., Chen, J. A. M. W., Gonzalez, C., Pople, Gaussian 03, (2003). http://www.gaussian.com.
[26] E. Cubero, F.J. Luque, M. Orozco, Is polarization important in cation-π interactions? Proc. Natl. Acad. Sci. 95 (1998) 5976–5980, http://dx.doi.org/10.1073/pnas.95.11.5976.
[27] G.D. Van Duyne, R.F. Standaert, S.L. Schreiber, J. Clardy, Atomic structure of the rapamycin human immunophilin FKBP-12 complex, J. Am. Chem. Soc. 113 (1991) 7433–7434, http://dx.doi.org/10.1021/ja00019a057.
[28] Ugo Varetto, Molekel Molecular Visualization, 2009, http://ugovaretto.github.io/molekel/wiki/pmwiki.php/Main/Citing.html.
[29] G.M. Morris, R. Huey, W. Lindstrom, M.F. Sanner, R.K. Belew, D.S. Goodsell, A.J. Olson, AutoDock4 and AutoDockTools4: automated docking with selective receptor flexibility, J. Comput. Chem. 30 (2009) 2785–2791, http://dx.doi.org/10.1002/jcc.21256.
[30] B. Szewczyk, A. Taylor, Diversity of Vi-related antigens in the microcapsule of Salmonella typhi, Infect. Immun. 30 (1980) 661–667.
[31] C.M. Soares, Estudo químico da alga Lithothamnion calcareum e avaliação da atividade inibitória do rolamento de leucócitos, UFMG, 2009, http://hdl.handle.net/1843/EMCO-7SMPDM.
[32] M. da S. Santos, C.L.O. Petkowicz, C.W.I. Haminiuk, L.M.B. Cândido, Polissacarídeos extraídos da gabiroba (Campomanesia xanthocarpa Berg): propriedades químicas e perfil reológico, Polímeros 20 (2010) 352–358, http://dx.doi.org/10.1590/S0104-14282010005000056.
[33] R.E. de Moura, Síntese de nanopartículas à base de goma do cajueiro para aplicação em sistemas de liberação de fármacos, Universidade Federal do Ceará, 2009, http://www.pgquim.ufc.br/wp-content/uploads/2011/11/DissertaçãoRAQUEL.pdf.
[34] E.J.J. Mallann, Obtenção de um no Composto Biológico com Porpiriedades Magnéticas, Universidade Federal do Ceará, 2010, http://www.pgquim.ufc.br/wp-content/uploads/2011/11/Disserta%C3%A7%C3%A3o-de-Mestrado-Eduardo-Jos%C3%A9-Juc%C3%A1-Mallmann.pdf.
[35] L.K. Shi-Shun, J.-M. Mallet, M. Moreau, P. Sinaÿ, Synthÿse dèoligomÿres du polysaccharide capsulaire de Salmonella typhi, bact'rie é l'origine de la fiÿvre typhoàde, Tetrahedron 55 (1999) 14043–14068, http://dx.doi.org/10.1016/S0040-4020(99)00869-8.
[36] L. Martínez, R. Andrade, E.G. Birgin, J.M. Martínez, PACKMOL: a package for building initial configurations for molecular dynamics simulations, J. Comput. Chem. 30 (2009) 2157–2164, http://dx.doi.org/10.1002/jcc.21224.